THE JOURNAL OF BIOLOGICAL CHEMISTRY VOL. 284, NO. 5, pp. 2978–2989, January 30, 2009

Amphetamine and Methamphetamine Differentially Affect Dopamine Transporters *in Vitro* and *in Vivo*[*][S]

Received for publication, July 11, 2008, and in revised form, November 25, 2008 Published, JBC Papers in Press, December 1, 2008, DOI 10.1074/jbc.M805298200

J. Shawn Goodwin[‡1], Gaynor A. Larson[§], Jarod Swant[¶], Namita Sen[‖], Jonathan A. Javitch[‖], Nancy R. Zahniser[§], Louis J. De Felice[‡‡], and Habibeh Khoshbouei[¶2]**

*From the Departments of [¶]Neurobiology and Neurotoxicology and [‡]Cancer Biology, Meharry Medical College, Nashville, Tennessee 37208, the [§]Department of Pharmacology, University of Colorado Denver, Aurora, Colorado 80045, the **Center for Molecular Neuroscience and [‡‡]Department of Pharmacology, Vanderbilt University, Nashville, Tennessee 37232, and the [‖]Departments of Psychiatry and Pharmacology, Center for Molecular Recognition, Columbia University, New York, New York 10027–6902*

The psychostimulants D-amphetamine (AMPH) and methamphetamine (METH) release excess dopamine (DA) into the synaptic clefts of dopaminergic neurons. Abnormal DA release is thought to occur by reverse transport through the DA transporter (DAT), and it is believed to underlie the severe behavioral effects of these drugs. Here we compare structurally similar AMPH and METH on DAT function in a heterologous expression system and in an animal model. In the *in vitro* expression system, DAT-mediated whole-cell currents were greater for METH stimulation than for AMPH. At the same voltage and concentration, METH released five times more DA than AMPH and did so at physiological membrane potentials. At maximally effective concentrations, METH released twice as much $[Ca^{2+}]_i$ from internal stores compared with AMPH. $[Ca^{2+}]_i$ responses to both drugs were independent of membrane voltage but inhibited by DAT antagonists. Intact phosphorylation sites in the N-terminal domain of DAT were required for the AMPH- and METH-induced increase in $[Ca^{2+}]_i$ and for the enhanced effects of METH on $[Ca^{2+}]_i$ elevation. Calmodulin-dependent protein kinase II and protein kinase C inhibitors alone or in combination also blocked AMPH- or METH-induced Ca^{2+} responses. Finally, in the rat nucleus accumbens, *in vivo* voltammetry showed that systemic application of METH inhibited DAT-mediated DA clearance more efficiently than AMPH, resulting in excess external DA. Together these data demonstrate that METH has a stronger effect on DAT-mediated cell physiology than AMPH, which may contribute to the euphoric and addictive properties of METH compared with AMPH.

The dopamine transporter (DAT)[3] is a main target for psychostimulants, such as D-amphetamine (AMPH), methamphetamine (METH), cocaine (COC), and methylphenidate (Ritalin®). DAT is the major clearance mechanism for synaptic dopamine (DA) (1) and thereby regulates the strength and duration of dopaminergic signaling. AMPH and METH are substrates for DAT and competitively inhibit DA uptake (2, 3) and release DA through reverse transport (4–9). AMPH- and METH-induced elevations in extracellular DA result in complex neurochemical changes and profound psychiatric effects (2, 10–16). Despite their structural and pharmacokinetic similarities, a recent National Institute on Drug Abuse report describes METH as a more potent stimulant than AMPH with longer lasting effects at comparable doses (17). Although the route of METH administration and its availability must contribute to the almost four times higher lifetime nonmedical use of METH compared with AMPH (18), there may also be differences in the mechanisms that underlie the actions of these two drugs on the dopamine transporter.

Recent studies by Joyce *et al.* (19) have shown that compared with D-AMPH alone, the combination of D- and L-AMPH in Adderall® significantly prolonged the time course of extracellular DA *in vivo*. These experiments demonstrate that subtle structural features of AMPH, such as chirality, can affect its action on dopamine transporters. Here we investigate whether METH, a more lipophilic analog of AMPH, affects DAT differently than AMPH, particularly in regard to stimulated DA efflux.

METH and AMPH have been reported as equally effective in increasing extracellular DA levels in rodent dorsal striatum (dSTR), nucleus accumbens (NAc) (10, 14, 20), striatal synaptosomes, and DAT-expressing cells *in vitro* (3, 6). John and

* This work was supported, in whole or in part, by National Institutes of Health Grants HL076133 (to J. S.), DA021471 (to H. K.), NS034075 and DA06338 (to L. J. D. F.), DA012408 and DA022413 (to J. A. J.), and DA004216 and DA015050 (to N. R. Z.). This work was also supported by National Science Foundation Award IOS-0642188 (to H. K.). Microscopy experiments and data analysis were performed through the use of the Meharry Medical College Morphology Core, which is supported in part by National Institutes of Health Grants U54NS041071, G12RR03032, U54CA91408, and U54RR019192. The costs of publication of this article were defrayed in part by the payment of page charges. This article must therefore be hereby marked "*advertisement*" in accordance with 18 U.S.C. Section 1734 solely to indicate this fact.

[S] The on-line version of this article (available at http://www.jbc.org) contains supplemental Fig. 1.

[1] Supported by National Institutes of Health Grant U54NS041071.

[2] To whom correspondence should be addressed: Meharry Medical College, Dept. of Neurobiology and Neurotoxicology, 3244 West Basic Science Bldg., 1005 Dr. D.B. Todd Jr. Blvd., Nashville, TN 37208. Tel.: 615-327-6472 (Office), 615-321-2948 (Lab); Fax: 615-327-6632.

[3] The abbreviations used are: DAT, human dopamine transporter; AMPH, D-amphetamine; METH, methamphetamine; COC, cocaine; DA, dopamine; NAc, nucleus accumbens; dSTR, dorsal striatum; CaMKII, calmodulin-dependent protein kinase II; KN93, 2-[*N*-(2-hydroxyethyl)]-*N*-(4-methoxybenzenesulfonyl)]amino-*N*-(4-chlorocinnamyl)-*N*-methylbenzylamine; KN92, inactive analog 2-[*N*-(4-methoxybenzenesulfonyl)]amino-*N*-(4-chlorocinnamyl)-*N*-methylbenzylamine; BIM, bisindolylmaleimide I; PKC, protein kinase C; YFP, yellow fluorescent protein; ANOVA, analysis of variance; FITC, fluorescein isothiocyanate.

Jones (21), however, have recently shown in mouse striatal and substantia nigra slices, that AMPH is a more potent inhibitor of DA uptake than METH. On the other hand, in synaptosomes METH inhibits DA uptake three times more effectively than AMPH (14), and in DAT-expressing COS-7 cells, METH releases DA more potently than AMPH (EC_{50} = 0.2 μM for METH *versus* EC_{50} = 1.7 μM for AMPH) (5). However, these differences do not hold up under all conditions. For example, in a study utilizing C6 cells, the disparity between AMPH and METH was not found (12).

The variations in AMPH and METH data extend to animal models. AMPH- and METH-mediated behavior has been reported as similar (22), lower (20), or higher (23) for AMPH compared with METH. Furthermore, although the maximal locomotor activation response was less for METH than for AMPH at a lower dose (2 mg/kg, intraperitoneal), both drugs decreased locomotor activity at a higher dose (4 mg/kg) (20). In contrast, in the presence of a salient stimuli, METH is more potent in increasing the overall magnitude of locomotor activity in rats yet is equipotent with AMPH in the absence of these stimuli (23).

The simultaneous regulation of DA uptake and efflux by DAT substrates such as AMPH and METH, as well as the voltage dependence of DAT (24), may confound the interpretation of existing data describing the action of these drugs. Our biophysical approaches allowed us to significantly decrease the contribution of DA uptake and more accurately determine DAT-mediated DA efflux with millisecond time resolution. We have thus exploited time-resolved, whole-cell voltage clamp in combination with *in vitro* and *in vivo* microamperometry and Ca^{2+} imaging to compare the impact of METH and AMPH on DAT function and determine the consequence of these interactions on cell physiology.

We find that near the resting potential, METH is more effective than AMPH in stimulating DAT to release DA. In addition, at efficacious concentrations METH generates more current, greater DA efflux, and higher Ca^{2+} release from internal stores than AMPH. Both METH-induced or the lesser AMPH-induced increase in intracellular Ca^{2+} are independent of membrane potential. The additional Ca^{2+} response induced by METH requires intact phosphorylation sites in the N-terminal domain of DAT. Finally, our *in vivo* voltammetry data indicate that METH inhibits clearance of locally applied DA more effectively than AMPH in the rat nucleus accumbens, which plays an important role in reward and addiction, but not in the dorsal striatum, which is involved in a variety of cognitive functions. Taken together these data imply that AMPH and METH have distinguishable effects on DAT that can be shown both at the molecular level and *in vivo*, and are likely to be implicated in the relative euphoric and addictive properties of these two psychostimulants.

MATERIALS AND METHODS

Reagents and drugs were purchased from Sigma unless otherwise noted.

Cell Lines and Cell Culture

The cell lines used in this study have been characterized previously (25–29). Briefly, a fluorescently tagged DAT was constructed by fusing the C terminus of the coding region of enhanced yellow fluorescent protein (YFP) from pEYFP-N1 (Clontech) to the N terminus of the human synthetic DAT cDNA, thereby creating the fusion construct YFP-DAT. Unless stated otherwise, YFP-DAT refers to YFP-tagged wild type DAT. This construct was subcloned into a bicistronic expression vector (30) modified to express the synthetic DAT from a cytomegalovirus promoter and the hygromycin resistance gene from an internal ribosomal entry site (pciHyg), as described previously (25, 28). EM4 cells, a HEK 293 cell line stably transfected with macrophage scavenger receptor (31), were transfected with YFP-DAT using Lipofectamine (Invitrogen), and a stably transfected pool (DAT cells) was selected in 250 μg/ml hygromycin as described previously (25, 28). Cells were grown in Dulbecco's modified Eagle's medium supplemented with 10% fetal bovine serum at 37 °C and 5% CO_2. Our previous studies have shown that addition of the N-terminal YFP tag does not alter the ability of the transporter to produce substrate-induced currents (25). In the YFP-DAT background, Ser-2, Ser-4, Ser-7, Ser-12, and Ser-13 were simultaneously mutated to alanine or aspartate in the YFP-S/A-DAT and YFP-S/D-DAT constructs, respectively (26). The mutant constructs were generated, confirmed, and expressed stably as described above. Our electrophysiological setup is equipped with the Nikon TE-2000U wide field microscope and filters that allow us to select cells for recording with maximum YFP signal and therefore human DAT expression. Parental nontransfected EM4 cells were used for control experiments. The EM4 cell line provides an appropriate parental background for studying DAT function because of the absence of DA uptake (32, 33) and the lack of substrate-induced whole-cell currents (25).

In Vitro Electrophysiology

Whole-cell Currents—Before recording from parental or stably expressing cells, cells were plated at 10^5 per 35-mm culture dish. Attached cells were washed three times with external solution at room temperature. The external solution contained 130 mM NaCl, 10 mM HEPES, 34 mM dextrose, 1.5 mM $CaCl_2$, 0.5 mM $MgSO_4$, and 1.3 mM KH_2PO_4 adjusted to pH 7.35 with a final osmolarity of 290 mosM. For measurement of the membrane potential as a function of external KCl, the osmolarity of the external solutions was controlled by decreasing the dextrose concentration in the external solution. The pipette solution for the whole-cell recording contained the following: 120 mM CsCl, 0.1 mM $CaCl_2$, 2 mM $MgCl_2$, 1.1 mM EGTA, 10 mM HEPES, and 30 mM dextrose plus 2 mM DA (when specified in the text)) adjusted to pH 7.35. The final osmolarity was 270 mosM.

Previously, we have demonstrated that DAT activity increases intracellular Na^+ and that a high concentration of Na^+ in the recording pipette increases DA efflux (25). Thus, to amplify DA efflux and to maintain an approximately constant Na^+ concentration inside the cell, the concentration of NaCl in

the pipette solution was increased to 30 mM in the presence or absence of 2 mM DA as specified in the text.

Patch electrodes were pulled from quartz pipettes on a P-2000 puller (Sutter Instruments, Novato, CA) and filled with the pipette solution. Whole-cell currents were recorded using an Axopatch 200B (Molecular Devices, Sunnyvale, CA) with a low-pass Bessel filter set at 1,000 Hz. Current-voltage relations were generated using a voltage step (500 ms) protocol ranging from −100 to +60 mV separated by 20 mV from a holding potential of −20 mV. Data were recorded and analyzed off-line using pCLAMP 9 software (Molecular Devices).

Amperometry—We monitored DA efflux simultaneously with whole-cell recording using an amperometric electrode (depicted in Fig. 3*A*). This amperometric carbon fiber electrode (ProCFE, Dagan Corp.), connected to a second amplifier (Axopatch 200B, Molecular Devices, Sunnyvale, CA), was attached to the plasma membrane of the cell and held at +700 mV, a potential greater than the redox potential of DA. The diameter of the carbon fiber electrode was 5 μm. An oxidative (amperometric) current-voltage relationship was generated as above. Unlike the usual amperometric calibration, which requires conversion to concentration, we report the current directly without considering the effective volume. Thus, our requirements are a defined base line, and our data represent a lower limit to the DA efflux, because some transmitter is lost to the bulk solution as described previously (25, 26).

Conversion of Amperometric Current to [DA]

Assume an electrode-gathering volume of 0.1 μm^3 that within this volume [DA] is constant for 1 ms and that one DA ion converts to 1 electron. Then 1 pA implies 0.625×10^4 DA molecules flow into the assumed volume in 1 ms. Under these assumptions, 1 pA converts to 100 μM DA and 0.01 pA converts to 1 μM DA. The amperometric currents were low pass filtered at 100 Hz. Data were recorded and analyzed off-line using pCLAMP 9 software. An upward deflection in the amperometric currents corresponds to an outward flux of DA. At the "on" of the voltage step, for voltages more positive than −40 mV, the amperometric electrode recorded an oxidation current (positive). This positive current is indicative of DA efflux. At the "off" of the voltage step, the amperometric current relaxed to base line. The on and off of the voltage step are defined by the *vertical arrows* in Fig. 3*A*, *right panel*. Moving the carbon fiber away from the patch caused the oxidative response to become smaller and slower. Furthermore, as expected for DA oxidation, the oxidative response diminished when we reduced the carbon fiber voltage to +300 mV and disappeared completely on further reduction.

For both whole-cell current and amperometry recordings, the DAT-mediated DA efflux was isolated by subtracting the current produced in the presence of cocaine from the base-line current (current produced in the absence of METH or AMPH). The METH- and AMPH-induced DA efflux were defined as the current recorded in the presence of the substrates (METH or AMPH), minus the current recorded after addition of cocaine to the bath with substrate still present. The steady-state current at a particular voltage was calculated as the average current during the final 100 ms of each potential tested. Plotting the steady-state current against the test voltage generated current-voltage ($I(V)$) relationships.

In Vivo Chronoamperometry

In vivo clearance of locally applied DA was measured in outbred male Sprague-Dawley rats ($n = 52$, mean weight = 262 ± 10 g; Charles River Laboratories, Wilmington, MA) using electrochemical methods described in detail elsewhere (34, 35). Animals were housed on a 12-h light/dark cycle (lights on at 0600 h) with *ad libitum* food and water. All animal-use procedures were in strict accordance with the National Institutes of Health Guide for the Care and Use of Laboratory Animals and were approved by the Institutional Animal Care and Use Committee at the University of Colorado, Denver.

Recording electrodes, calibrated *in vitro* for their response to DA, consisted of a single 30-μm diameter Nafion-coated carbon fiber. A calibrated electrode was attached to a single-barrel pipette loaded with 200 mM DA, 100 mM ascorbic acid (pH 7.4). Rats were anesthetized with urethane (1.25–1.5 g/kg, intraperitoneal), and electrode/pipette assemblies were lowered under stereotaxic control into a single location (1.5 mm anterior, 2.2 mm lateral with respect to bregma) in either dSTR (3.8-4.9 mm ventral with respect to the brain surface) or NAc (6.5–8.0 mm ventral) (36). An Ag/AgCl reference electrode was lowered just anterior to the interaural line into the cerebral cortex. Chronoamperometric measurements were made using an IVEC-10 system (Quanteon, LLC, Lexington, KY), which applied square-wave pulses of 0.00–0.55 V (with respect to reference) at a frequency of 5 Hz. Resulting oxidation (and reduction) currents were digitally integrated, and changes in DA oxidation signals were expressed quantitatively based on the *in vitro* calibration.

For all *in vivo* chronoamperometry experiments, the background current was set to zero prior to pressure-ejecting DA (10–22 p.s.i. for 0.1–4.0 s) at calibrated volumes (96 ± 10 nl). For a given assembly, an ejection volume was chosen that resulted in signal amplitudes of 1.0–3.7 μM. Ejections were made at 5-min intervals, and a base line was established when signal amplitude varied by ≤15% for two consecutive applications. Volumes were monitored for consistency during each DA application and were not altered within a given experiment. After measures of base-line DA clearance (DAT function) were obtained, rats were injected with either 1 or 5 mg/kg AMPH or METH (intraperitoneal) 1 min prior to $t = 0$. DA ejections were continued at 5-min intervals for 60 min. All recording sites were confirmed histologically.

Two signal parameters were analyzed from the DA oxidation currents as follows: maximal signal amplitude (A_{max}) and signal time course (T_{80}; the time for the signal to rise to A_{max} and then decay by 80%). Each data set was normalized by obtaining a mean value for parameters during the two-point base-line period, setting this value to 100%, and expressing all data as a percentage of this base-line value.

Intracellular Calcium Mobilization

Cells stably expressing YFP-DAT, YFP-S/A-DAT, YFP-S/D-DAT, or parental nontransfected EM4 cells were plated on glass bottom microwell dishes (MatTek Corp., Ashland, MA) 48 h

before the experiments. Cells were loaded with the cell-permeant, Ca^{2+}-sensitive dye Fura 2-AM (5 μM) (Molecular Probes, Carlsbad, CA) for 30 min at 37 °C, washed three times in external solution, and acclimated to room temperature for 10 min. The dishes were mounted on an inverted Nikon TE2000E microscope at room temperature. Images were collected using a 40×, 1.3 NA, oil immersion Plan Fluor objective lens, and a side-mounted CoolSNAPHQ$_2$ camera. Fluorescence was monitored using dual excitation wavelengths (340/380 nm) and a single emission wavelength (510 nm). Fluorescence at 340 nm indicates dye bound to Ca^{2+}, whereas that at 380 nm corresponds to free dye. Basal readings were taken for 60 s before addition of METH or AMPH (10 μM). In some experiments cells were incubated with either COC (10 μM), thapsigargin (2 μM), or $CdCl_2$ (2 mM) for 5 min before stimulation of the cells with AMPH or METH. Nikon Elements Advanced Research imaging software (Nikon Instruments) was used for automated collection of images at ~1-s intervals over a 5-min period. During this time, cells maintained a healthy morphology.

Images of cells expressing YFP-DAT were taken with a FITC HyQ filter cube before and after the addition of METH or AMPH. Only cells expressing detectable YFP-DAT signals were included in the analysis. Average fluorescence measurements were determined using Nikon Elements software. Data are expressed as the ratio of bound:free (340/380 values) Fura 2-AM fluorescence intensities after background subtraction. For time-matched statistical analysis, the Ca^{2+} levels were normalized to the average fluorescence intensities (340/380 values) of basal values (first 60 images).

As a positive control for cell viability and for FURA-2 AM function, 5 μM ionomycin was added at the termination of all calcium mobilization assays. More than 95% of the cells exhibited a rapid increase in internal Ca^{2+} in response to ionomycin, and only ionomycin-sensitive cells were included in the analysis.

Statistical Analysis

The data are expressed as mean values ± S.E. For most of the results, GraphPad Prism 4 was used to determine statistical significance. ANOVA with post hoc Newman-Keuls was used for the statistical comparison of more than two means. The two-tailed, unpaired Student's *t* test was applied when two means were compared. The *in vivo* chronoamperometry results were analyzed using three-way ANOVA (SigmaStat) followed by Tukey post hoc analysis.

RESULTS

Quantification of DAT-induced Depolarization in HEK Cells—First, we investigated the electrogenic properties of DAT (24) and the impact of the leak current on membrane potential by comparing DAT-expressing cells with nontransfected parental cells. The cells were held at −20 mV and stepped in 20-mV increments from −100 to +60 mV. For the *in vitro* electrophysiology experiments, we empirically selected a holding potential of −20 mV, which improves the integrity of the cells and keeps them viable for up to 1 h. More negative holding potentials produce significant background inward current, and by holding at −20 mV and briefly probing more negative potentials, we more accurately assessed differences in AMPH- and METH-stimulated effects on human DAT. Fig. 1*A* shows the current-voltage relationships for parental *versus* DAT-expressing cells. Both data sets are shown after subtraction of currents measured in the presence of 10 μM COC, a DAT inhibitor. Parental cells displayed a COC-insensitive whole-cell current, whereas DAT-transfected cells displayed a constitutive COC-sensitive current.

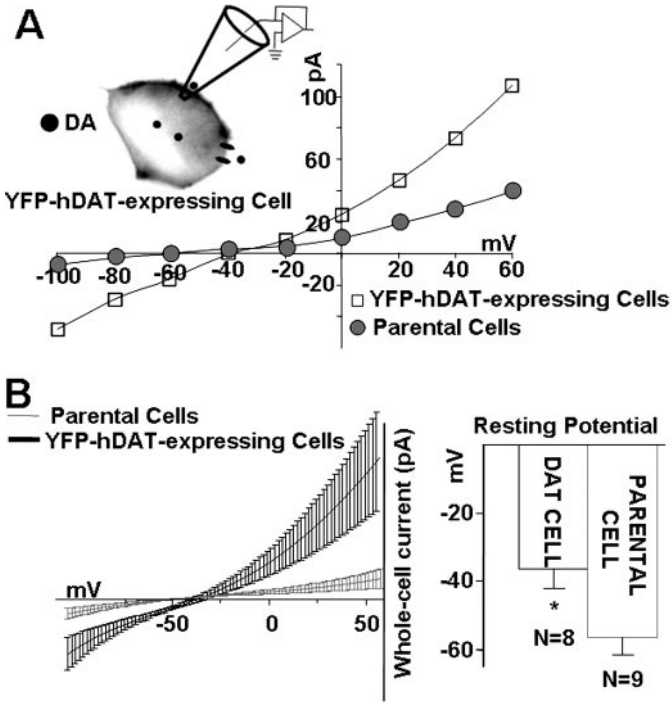

FIGURE 1. **Expression of DAT constitutively depolarizes cells.** *A*, representative current-voltage (*I*(*V*)) relationships of DAT-mediated currents in DAT-expressing cells (*open squares*) compared with *I*(*V*) relationships in parental, nontransfected cells (*closed circles*). Cells were voltage-clamped with a whole-cell patch pipette containing 30 mM Na^+ without DA present inside or outside the cells (see "Materials and Methods"). Whole-cell currents were obtained by stepping the membrane potential in −20 mV steps between −100 to +60 mV, from a holding potential of −20 mV. The *I*(*V*) curves were obtained after subtracting currents in the presence of 10 μM of the DAT inhibitor, cocaine (see "Materials and Methods"). *B, left panel* shows the expansion of *A* near the two reversal potentials. The *I*(*V*) curves were fit to polynomials (*solid lines*) from the reversal potentials (n = 8–9). *Right panel* depicts *bar graphs* of the mean resting potentials measured in DAT-transfected cells (−36.5 ± 5.5) and parental nontransfected cells (−56.3 ± 4.7) $p < 0.05$.

The average values of the currents recorded from DAT-expressing cells *versus* parental cells were profoundly different. At +60 mV, the current recorded in parental cells was 32.5 ± 13.6 pA, n = 9, whereas in DAT-expressing cells it was 118.9 ± 30.7 pA, n = 8 ($p < 0.05$) (Fig. 1*A*). At −60 mV, the current in parental cells was −0.25 ± 2.9 pA, n = 9, and in DAT-expressing cells it was −18.1 ± 1.7 pA, n = 8 ($p < 0.05$) (Fig. 1*A*). Interestingly, parental cells have a resting potential of −56.3 ± 4.7 mV, whereas the resting potential in DAT-expressing cells was −36.5 ± 5.5 mV ($p < 0.05$) (Fig. 1*B*). Thus, even in the absence of DA, the presence of DAT at the plasma membrane of YFP-DAT-expressing cells depolarizes the cells. This finding is consistent with the presence of a well characterized endogenous DAT leak current in the absence of the substrate (24).

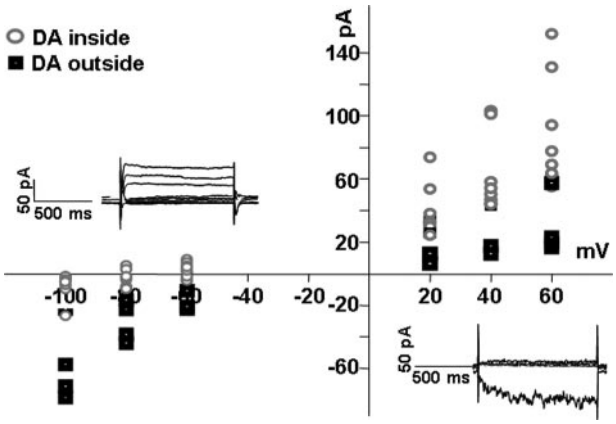

FIGURE 2. **Translocation of DA through DAT produces current.** Cells were voltage-clamped with a whole-cell patch pipette containing 30 mM Na^+ with or without 2 mM DA. Whole-cell currents were obtained by stepping the membrane potential in −20-mV steps between −100 to +60 mV, from a holding potential of −20 mV. The *I*(*V*) curves were obtained after subtracting currents in the presence of 10 μM cocaine (see "Materials and Methods"). *Insets* show raw whole-cell currents when DA was added to the bath solution (*lower right*) or pipette solution (*upper left*). The *I*(*V*) curve for 2 mM DA outside the cells shows a dominant inward current (*solid squares*), and the *I*(*V*) curve for 2 mM DA inside the cells shows a dominant outward current (*open circles*).

Direction of DAT-mediated, DA-induced Currents Depends on Whether DA Is Inside or Outside the Cell—We found that exposure of DAT-expressing cells to DA produces currents, and that the direction of these currents differs when DA is present inside *versus* outside the cells. As shown in Fig. 2, bath application of 2 mM DA generated inward currents in DAT-expressing cells (*closed squares*) consistent with previous findings (24), and when DA was perfused into these cells via a whole-cell pipette, it generated outward currents (*open circles*). Both of these currents were inhibited by bath application of 10 μM COC, and neither of these DA-dependent currents was detected in parental cells (data not shown). It is also of interest that intracellular application of DA shifted the reversal potential of the DAT-dependent currents to more negative potentials, whereas extracellular (*i.e.* bath) application of DA shifted the reversal potential to more positive potentials, consistent with the direction of current.

METH Is More Effective than AMPH in Releasing DA—Extracellular levels of METH in the rat striatum, contingent on the route, regimen, and dose of METH administration, could be in the range of ~5 μM (37–39). Thus, we compared the ability of METH and AMPH to modify DAT-mediated whole-cell currents and DA efflux at multiple concentrations within this range. We used a combination of patch clamp and amperometry, as shown schematically in Fig. 3*A* and described in detail under "Materials and Methods." The oxidative current has been shown to be a quantitative measure of the release of DA in this preparation (see "Materials and Methods"). The *vertical arrows* in the *right-hand panel* of Fig. 3*A* indicate the on and off of voltage steps in our protocol, and the representative traces in this panel reflect changes in both whole-cell and oxidative currents. Stepping from a holding potential of −20 mV to more positive voltages increased the oxidative currents (DA efflux). Returning to the holding potential decreased the oxidative currents, which returned to base line. Fig. 3*B* demonstrates that at a constant voltage of +60 mV METH was both more potent and

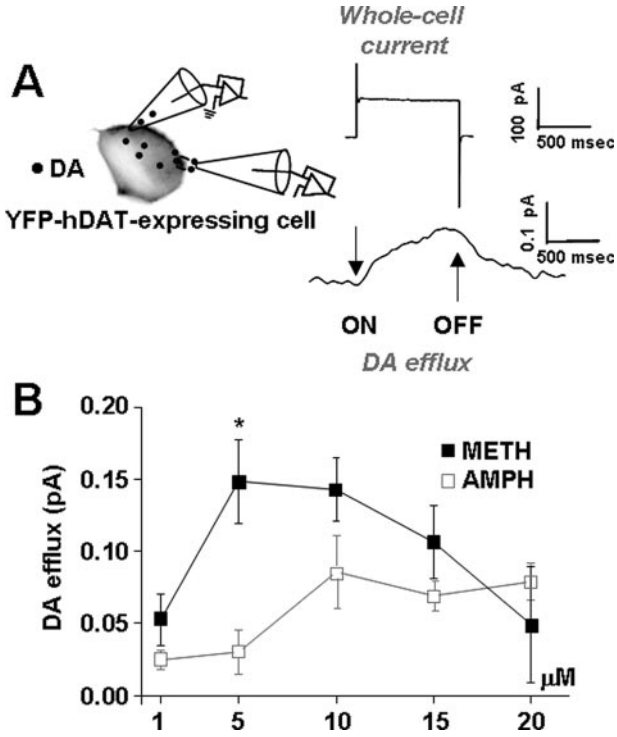

FIGURE 3. **At lower concentrations METH is more effective in releasing DA.** *A*, DAT-transfected cells were voltage-clamped, and simultaneously, an amperometric electrode was placed on the cell membrane to monitor DA release via oxidative current. DAT-mediated currents (whole-cell and oxidative) were recorded by stepping the whole-cell electrode between −100 and +60 mV from a holding potential of −20 mV. The amperometric electrode was held at +700 mV to measure DA oxidation. An upward deflection represents DA efflux. *B*, DA efflux stimulated by 1, 5, 10, 15, or 20 μM AMPH or METH when the membrane potential was held at +60 mV ($p < 0.05$).

more efficacious than AMPH in promoting DA release. Thus, 5 μM METH under depolarizing conditions led to five times more DA release than with 5 μM AMPH ($p < 0.05$). At concentrations above 10 μM, METH-mediated DA efflux decreased. It is possible that METH desensitizes the transporter at these higher concentrations or activates systems with an ancillary inhibitory effect on DA efflux. Future studies will be needed to examine these possibilities. Because METH and AMPH were both maximally effective in releasing DA at 10 μM, we used 10 μM AMPH and METH throughout the remainder of this study. Furthermore, 10 μM AMPH has been extensively used to assess human DAT-mediated functions, including changes in intracellular Na^+, DA efflux, and whole-cell currents (25–27, 33, 40).

Compared with AMPH, METH Stimulates More DA Efflux, and It Does So at More Negative Membrane Potentials—Fig. 4*A* demonstrates that 10 μM METH evoked dramatically enhanced outward currents compared with 10 μM AMPH. METH-induced current reversed at more negative membrane potentials. METH-induced whole-cell currents reversed at −44.2 ± 0.68 mV, whereas AMPH-induced current reversed at −17.5 ± 2.08 mV ($p < 0.05$). The marked increase in whole-cell currents in response to METH compared with AMPH was paralleled by dramatic differences in oxidative currents, a measure of DA efflux, evoked by these agents. METH produced a significantly higher increase in DAT-mediated DA efflux at positive voltages ($p < 0.05$) (Fig. 4*A*). Furthermore, similar to whole-cell currents, oxidative currents evoked by METH were initiated at a

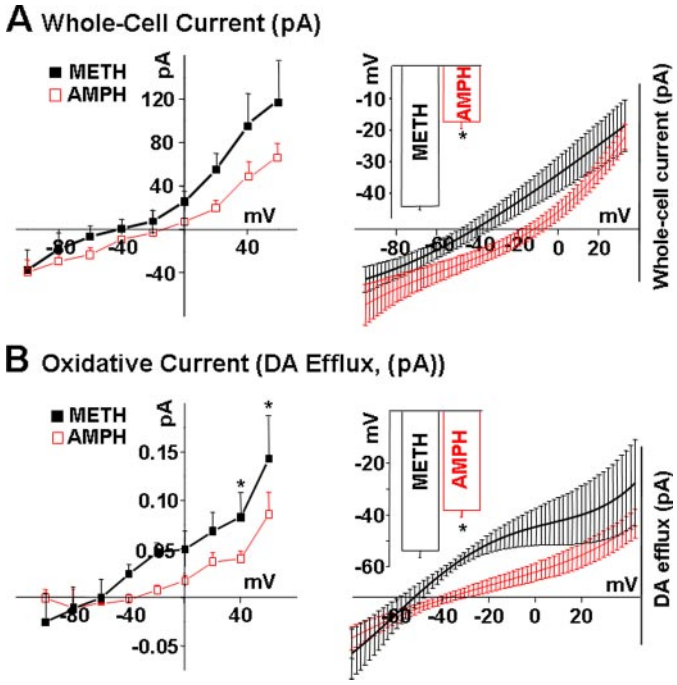

FIGURE 4. **METH releases more DA from DAT-transfected cells.** Experiments were performed as described in Fig. 3 with the difference that we used a fixed concentration of 10 μM AMPH or METH. *A,* METH increases in DAT-mediated whole-cell currents at all voltages compared with AMPH ($p < 0.05$). The *right panel* shows the expansion of *A* near the two reversal potentials fit to polynomials (*solid lines*). METH-induced whole-cell current reversed at -44.2 ± 0.68 (*thick line*), whereas AMPH-induced current reversed at -17.5 ± 2.08 (*thin line*) ($n = 7–9$, $p < 0.05$). *B,* METH mediates significantly greater DA efflux compared with AMPH. The *right panel* depicts the expansion of *B* near the two reversal potentials fit to polynomials (*solid lines*). For METH, the oxidative current initiated at -58.38 ± 0.8 (*thick line*), whereas the AMPH-mediated oxidative current initiated at -38.42 ± 0.3 (*thin line*) ($n = 7–9$ $p < 0.05$).

lower membrane potential, -58.38 ± 0.08 mV for METH compared with -38.42 ± 0.03 mV for AMPH ($p < 0.05$) (Fig. 4*B*). Thus, METH-mediated DA efflux far exceeded that following AMPH stimulation, and the reversal potential for DA efflux was significantly more negative for METH than AMPH. This finding could be of considerable physiological importance, because the onset of METH-induced DA efflux occurred nearer the resting potential of neuronal cells (approximately −70 mV) and thus required less depolarization compared with AMPH-induced DA efflux.

In Rat NAc, METH Inhibits DAT-mediated DA Clearance More Effectively than AMPH—The clearance of locally applied DA, as measured with chronoamperometry in dSTR or NAc of urethane-anesthetized rats, is largely mediated by DAT (41, 42). Here we found that inhibition of *in vivo* DA clearance in NAc, as measured by increased DA clearance time (T_{80}), was similar following an intraperitoneal injection of 1 mg/kg AMPH or METH but was significantly greater following 5 mg/kg METH than AMPH (Fig. 5*A*). Three-way ANOVA revealed a significant main effect of drug ($F(1, 144) = 40.6$, $p < 0.001$) and dose ($F(1, 144) = 81.5$, $p < 0.001$) and a drug × dose interaction ($F(11, 144) = 39.7$, $p < 0.001$). Subsequent post hoc Tukey tests revealed a significant difference between METH and AMPH at 5 mg/kg ($p < 0.001$) but not at 1 mg/kg ($p = 0.959$). In contrast, the 1 mg/kg dose of AMPH or METH did not alter DA signal amplitude (A_{max}), and 5 mg/kg of either

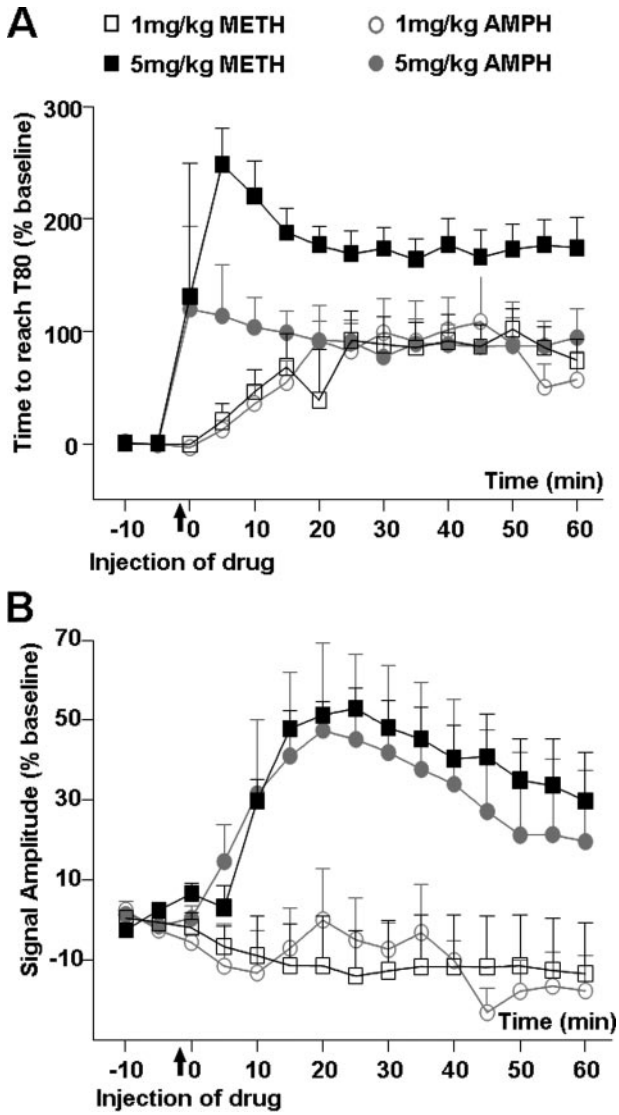

FIGURE 5. **METH is a more effective inhibitor than AMPH of *in vivo* DAT activity in rat NAc.** Chronoamperometry was used to measure clearance of DA, locally applied every 5 min, in NAc of urethane-anesthetized rats. Mean values ± S.E. for $n = 4$/group are shown and expressed as a percent of their respective base-line values. Drugs (AMPH or METH, 1 or 5 mg/kg) were injected intraperitoneally 1 min before time = 0. *A,* DA clearance time (T_{80}) was increased to the same extent by 1 mg/kg AMPH or METH, but was increased to a greater extent by 5 mg/kg METH than AMPH. *B,* DA signal amplitude (A_{max}) was not altered by 1 mg/kg AMPH or METH and was increased similarly by 5 mg/kg AMPH or METH.

drug increased A_{max} to the same extent (Fig. 5*B*). Also, no significant differences in AMPH- *versus* METH-induced changes in DA clearance time (T_{80}) were observed in dSTR with either drug dose (supplemental Fig. 1). The lack of differences between AMPH and METH on DA clearance time (T_{80}) in dSTR is significant because systemic AMPH or METH releases DA in the nucleus accumbens and increases locomotor activity (10). In addition, elevated DA in the nucleus accumbens is essential to the development of drug addiction (43).

METH Stimulates a Greater Increase in $[Ca^{2+}]_i$ Levels than AMPH—Previously, we have shown that buffering $[Ca^{2+}]_i$ abolishes AMPH-stimulated DA efflux, suggesting that changes in $[Ca^{2+}]_i$ serve as an intracellular trigger for DAT-evoked DA efflux (26). Consequently, we evaluated the impact

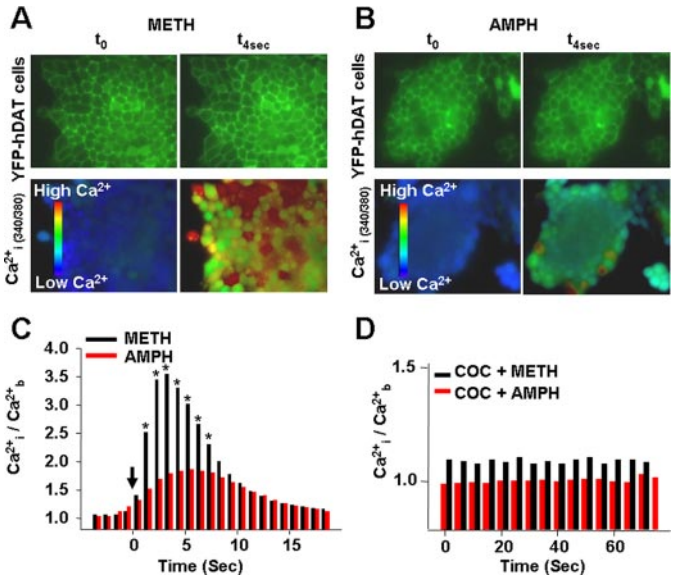

FIGURE 6. **METH causes greater increases in intracellular Ca^{2+} than AMPH.** DAT-expressing cells exposed to METH (*A*) or AMPH (*B*) at $t = 0$ and 4 s. Basal fluorescence readings were taken for 60 s (~60 images) before stimulation with either METH (10 μM) or AMPH (10 μM) as described under "Materials and Methods" ($[Ca^{2+}]_b$). *C*, internal free Ca^{2+} ($[Ca^{2+}]_i$) after adding 10 μM METH or AMPH (*solid arrow*) to the DAT-expressing cells; $n = 97–151$ cells measured in 3–5 independent experiments ($0.001 < p < 0.05$). *D*, cocaine pretreatment blocks the effect of METH and AMPH on $[Ca^{2+}]_i$.

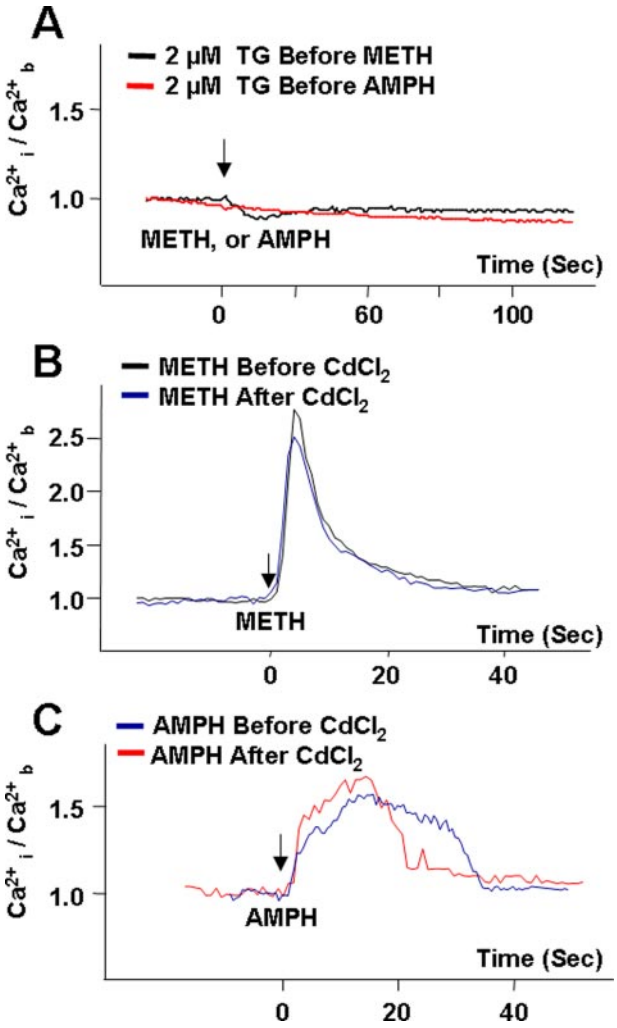

FIGURE 7. **AMPH- and METH-mediated $[Ca^{2+}]_i$ increase is derived from thapsigargin-sensitive internal stores, not $CdCl_2$-sensitive plasma membrane calcium channels.** *A*, representative experiment showing incubation of DAT-expressing cells with 2 μM thapsigargin (*TG*) eliminated the Ca^{2+} response induced by both AMPH and METH; $n = 30–57$ cells recorded in 2–3 independent experiments for each condition. *B* and *C* are representative experiments showing the presence of a non-subtype selective Ca^{2+} channel blocker (2 mM $CdCl_2$) had no impact on METH-mediated increases (*B*, $n = 106$ in four independent experiments) or AMPH-mediated increases (*C*, $n = 57$ in three independent experiments) in internal free Ca^{2+} ($[Ca^{2+}]_i$). *Solid arrows* indicate addition of the stimulants. Values were normalized to the average basal values ($[Ca^{2+}]_b$) for each independent experiment.

of METH *versus* AMPH on changes in $[Ca^{2+}]_i$. The *top panels* in Fig. 6, *A* and *B*, are images of YFP-DAT-expressing cells at time 0 (t_0) and 4 s after METH or AMPH were added (t_{4s}) using a FITC HyQ filter cube. The *two bottom panels* in Fig. 6, *A* and *B*, are images of the same cells containing Fura-2, and they show $[Ca^{2+}]_i$ levels at time 0 (t_0) and 4 s after METH or AMPH were added (t_{4s}). As shown in Fig. 6, *A–C*, METH produced more than twice as great an increase in $[Ca^{2+}]_i$ compared with AMPH ($p < 0.05$, $n = 97–151$ measurements from 3 to 5 independent experiments for each treatment). Thus, at their most effective concentrations for DA release, METH elevated $[Ca^{2+}]_i$ substantially more than AMPH. In both cases, these changes were blocked by prior exposure to COC, indicating that the increases in $[Ca^{2+}]_i$ were dependent on METH and AMPH interactions with DAT (Fig. 6*D*) ($n = 90$ cells in three independent experiments).

AMPH- and METH-induced Elevation in $[Ca^{2+}]_i$ Are from Internal Stores—We next determined whether elevations in $[Ca^{2+}]_i$ were from intra- or extracellular stores. Ca^{2+} release from internal stores is eliminated by thapsigargin (44–46), whereas exposure to Cd^{2+} blocks Ca^{2+} channels at the plasma membrane (47, 48), eliminating Ca^{2+} contribution from the extracellular environment. As shown in Fig. 7*A*, pre-exposure of DAT-expressing cells to 2 μM thapsigargin abolished the ability of both METH and AMPH to increase $[Ca^{2+}]_i$. The addition of 5 μM ionomycin, a Ca^{2+} ionophore, to the bath solution at the end of each experiment with thapsigargin produced a rapid increase in $[Ca^{2+}]_i$ (data not shown), indicating that elimination of the Ca^{2+} signal by thapsigargin was not because of perturbed fluorophore functioning or altered cell viability (see "Materials and Methods"), but indeed represented the role of thapsigargin-sensitive intracellular Ca^{2+} pools in the METH- and AMPH-elicited increase in intracellular Ca^{2+}. In contrast to the effect of thapsigargin, pretreatment with 2 mM $CdCl_2$ did not block the 10 μM METH- (Fig. 7*B*) or AMPH-stimulated (Fig. 7*C*) Ca^{2+} responses.

In the experiments where the cells were treated with thapsigargin, basal intracellular Ca^{2+} was not affected (data not shown). However, 2 mM $CdCl_2$ introduced an upward drift in the absence of stimulants in both parental and DAT-expressing cells (data not shown). Therefore, in experiments where a $CdCl_2$ effect was assessed, the values obtained for $CdCl_2$-only treatments were subtracted from the stimulus-induced Ca^{2+} response.

These results are consistent with previous reports that at high concentrations of AMPH (*e.g.* 100 μM) the increase of $[Ca^{2+}]_i$ was independent of the presence of extracellular Ca^{2+}

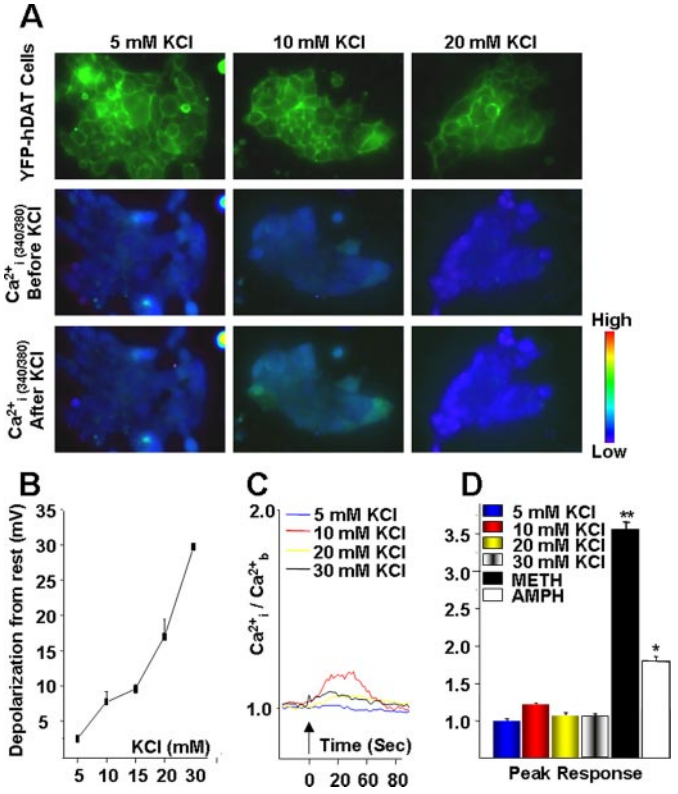

FIGURE 8. **Membrane depolarization does not contribute to rise in $[Ca^{2+}]_i$.** *A, top panel* is an image of YFP-DAT-expressing cells at time zero (t_0) using a FITC HyQ filter cube. *Middle* and *lower panels* depict changes in internal free Ca^{2+} ($[Ca^{2+}]_i$), from a single representative experiment recorded at 0 s (*middle panel*) and ~10 s (*lower panel*, peak response) after stimulation with 10 mM KCl. *B,* membrane potential changes as a function of external [KCl]. Cells were patched in the whole-cell configuration, and the membrane potentials were measured in varying levels of [KCl] (n = 3–5 cells for each KCl concentration). External solutions were controlled for osmolarity (see under "Materials and Methods"). *C,* representative quantitative increase in $[Ca^{2+}]_i$ after stimulation with 5, 10, 20, and 30 mM KCl as shown in *B* as a function of time. The entire experiment was recorded for 5 min, and $[Ca^{2+}]_i$ response was only seen immediately after KCl addition. Values were normalized to the average basal values ($[Ca^{2+}]_b$) for each independent experiment. *D, bar graph* represents peak $[Ca^{2+}]_i$ responses observed at ~10 s after stimulation with varying KCl concentrations (n = 31–64 cells of three independent experiments for each concentration) and compared with findings observed following stimulation with 10 μM AMPH or METH, $p > 0.05$ (see Fig. 6).

(26), and the results support the interpretation that, under the conditions tested, AMPH and METH-induced elevations of intracellular $[Ca^{2+}]$ were derived almost exclusively from internal stores.

Membrane Depolarization Does Not Contribute to the AMPH- or METH-induced Rise in $[Ca^{2+}]_i$—Because AMPH induces an appreciable Na^+-dependent inward current that increases $[Na^+]_i$ and depolarizes cells through a DAT-dependent mechanism (25), it is possible that DAT-mediated depolarization may contribute to the elevation of $[Ca^{2+}]_i$. To test this possibility directly, we generated a wide range of membrane potentials by varying levels of external KCl ($[KCl]_{ext}$), while controlling extracellular osmolarity. Thus, we examined depolarization-induced changes in $[Ca^{2+}]_i$. As shown in Fig. 8*B*, the membrane potential of DAT-expressing cells varied smoothly as a function of $[KCl]_{ext}$ (n = 3–5). Increasing $[KCl]_{ext}$ from 2.4 mM (control) to 5, 10, 15, 20, and 30 mM depolarized the membrane by 2.46 ± 0.35 mV, 7.72 ± 1.46 mV, 9.55 ± 0.61 mV, 16.98 ± 2.42 mV, and 29.70 ± 1.41 mV, respectively. For comparison, the mean resting potential in the control condition (without altered KCl_{ext}) was −26.9 ± 4.2 mV. As shown in Fig. 8, *A*, *C,* and *D,* increasing $[KCl]_{ext}$ and thus incrementally depolarizing DAT-expressing cells caused some transient and local changes in $[Ca^{2+}]_i$, but these were small compared with the changes seen in response to AMPH or METH under control conditions (Fig. 8*D*). Relative to base line (before addition of the drug), the $[Ca^{2+}]_i$ levels after bath application of 5, 10, 20, and 30 mM KCl were 0.013 ± 0.0133, 0.18 ± 0.0808, 0.06 ± 0.0275, and 0.08 ± 0.029, respectively (Fig. 8, *C* and *D*). The small increase (0.18-fold above base line) in $[Ca^{2+}]_i$ after prolonged bath application of 10 mM KCl was likely because of voltage-activated Ca^{2+} channels. Therefore, although DAT-mediated DA efflux was voltage-dependent (25), depolarization did not elevate $[Ca^{2+}]_i$ to levels comparable with those induced by AMPH or METH (Fig. 8*D*).

An Intact N-terminal Domain of DAT Is Required for the AMPH- and METH-induced Increase in $[Ca^{2+}]_i$ and for the Enhanced Effects of METH on $[Ca^{2+}]_i$—Cervinski *et al.* (49) have shown that the N-terminal serines on rat DAT are required for METH-induced DAT phosphorylation but not for METH-induced down-regulation of the transporter, and that removal of the first 22 residues of DAT containing the N-terminal serine cluster prevents PKC-induced DAT phosphorylation but not its down-regulation or endocytosis. We have shown that mutation of N-terminal serines (Ser-2, -4, -7, -12, and -13) to alanine in DAT (referred to as S/A-DAT) blunts AMPH-induced, DAT-mediated DA efflux, whereas mutation to aspartate (referred to as S/D-DAT) restored the AMPH-mediated efflux without an additional increase from basal (26). Nevertheless, both mutant structures are targeted properly to the plasma membrane, possess normal substrate uptake, cocaine binding, and transporter oligomerization (26, 50, 51).

Because our previous findings had demonstrated a decrease in basal and AMPH-evoked DA efflux in S/A-DAT, it was of interest to determine whether S/A-DAT affected METH- or AMPH-stimulated elevations in intracellular Ca^{2+}. As shown in Fig. 9*A*, mutation of these five N-terminal serines to alanine decreased both AMPH- and METH-induced $[Ca^{2+}]_i$ elevations characteristic of the YFP-tagged wild type DAT-expressing cells. Of considerable interest is that in S/A-DAT cells, there was no significant difference between AMPH- and METH-meditated increase in $[Ca^{2+}]_i$. Similar to our previous report that S/D-DAT-expressing cells only restored the AMPH-mediated DA efflux (26), the AMPH- and METH-mediated increase in $[Ca^{2+}]_i$ in S/D-DAT cells was similar to levels stimulated by AMPH in wild type DAT cells (Fig. 9*A*) (n = 60–147 cells in three independent experiments). Therefore, N-terminal phosphorylation likely regulates DAT-mediated $[Ca^{2+}]_i$ increases, consistent with other DAT functions (26, 49–51).

PKC and CaMKII Are Required for AMPH- and METH-mediated Increase in $[Ca^{2+}]_i$—A large body of literature supports regulatory roles for protein kinases and suggests that DAT phosphorylation affects its function (52–60). Specifically, Cervinski *et al.* (49) reported that METH (at the same dose used in this study, 10 μM) and AMPH (2 μM), as well as protein kinase C activation, stimulate rat DAT phosphorylation and decrease

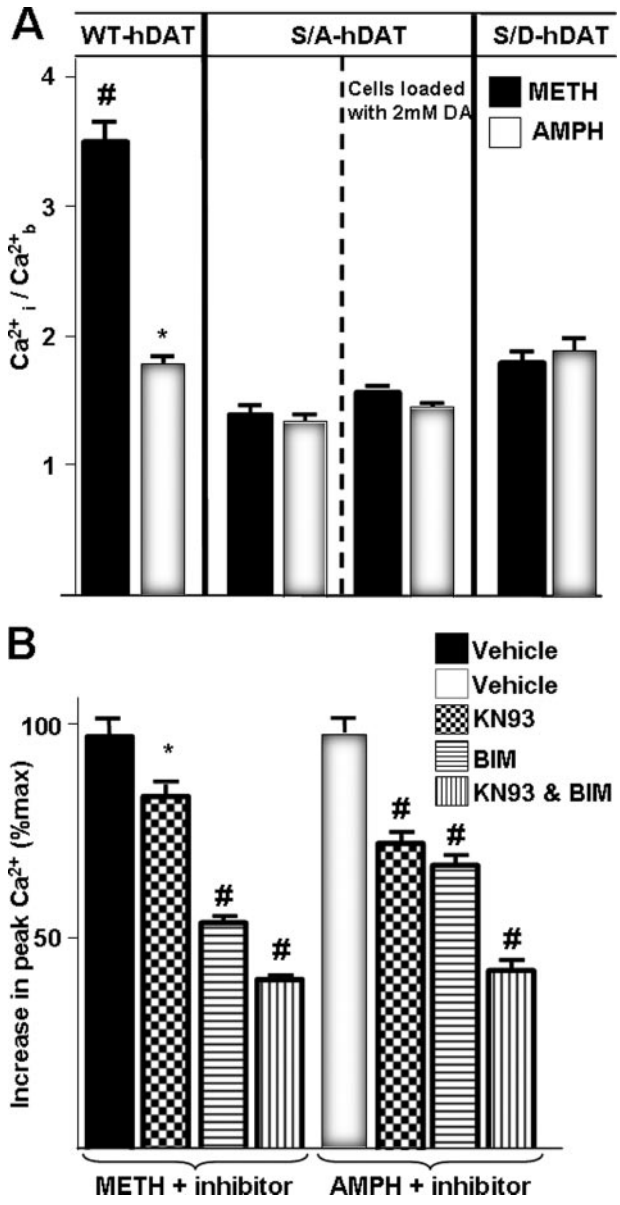

FIGURE 9. **N-terminal phosphorylation sites of DAT are necessary for the METH-mediated elevation of $[Ca^{2+}]_i$.** *A, bar graph* represents peak $[Ca^{2+}]_i$ responses observed following stimulation with 10 μM AMPH or METH in YFP-DAT, S/A DAT, and S/D DAT cells (#, *, $p < 0.05$ for METH- and AMPH-treated groups, respectively, compared with other groups). *B,* cells were mock-pretreated or pretreated with 10 μM kinase inhibitors (KN93, BIM, or both) for 10 min. The *bar graph* depicts percent change from maximum peak Ca^{2+} response to 10 μM METH or AMPH (*, $p > 0.05$; #, $p < 0.05$) ($n = 37–147$ cells of at least 2–3 independent experiments for each condition). Values were normalized to the average basal values for each independent experiment, and percent changes from maximum increase in peak Ca^{2+} levels after the addition of 10 μM METH (*B, left panel*) or AMPH (*B, right panel*) are reported.

basal [^{3}H]DA uptake. Therefore, we asked whether activation of CaMKII and/or PKC was necessary for the Ca^{2+} responses stimulated by AMPH and METH. Incubation of FURA-2-loaded cells with 10 μM 2-[*N*-(2-hydroxyethyl)]-*N*-(4-methoxybenzenesulfonyl)]amino-*N*-(4-chlorocinnamyl)-*N*-methylbenzylamine (KN93), a CaMKII inhibitor, or 10 μM bisindolylmaleimide I (BIM), a PKC inhibitor, for 10 min partially attenuated the AMPH- and METH-mediated increase in intracellular $[Ca^{2+}]_i$. Moreover, the METH- or AMPH-mediated increase in intracellular $[Ca^{2+}]_i$ was blocked altogether when the cells were incubated with both inhibitors (Fig. 9*B*) ($n = 93–127$ cells in two to three independent experiments) ($p < 0.05$). This is consistent with previous findings that AMPH-induced DA efflux was decreased by a CaMKII inhibitor, and METH-stimulated DAT phosphorylation was decreased by BIM (49, 52, 55, 56, 61–63) at the same dose (49) used in our study. The inactive analog of KN93, 2-[*N*-(4-methoxybenzenesulfonyl)]amino-*N*-(4-chlorocinnamyl)-*N*-methylbenzylamine (KN92) had no effect on basal intracellular Ca^{2+} levels, or the AMPH- and METH-stimulated changes in intracellular Ca^{2+} (data not shown).

Differences in METH- and AMPH-evoked $[Ca^{2+}]_i$ Are Not Modulated by $[DA]_i$—It is possible that intracellular DA changes DAT activity independent of N-terminal phosphorylation, thus altering AMPH- and METH-stimulated Ca^{2+} responses. Therefore, we measured Ca^{2+} responses in YFP-DAT cells when DA was present intracellularly. As shown in Fig. 9*A*, intracellular DA (2 mM) did not restore the METH-induced Ca^{2+} response to that of wild type DAT-expressing cells, nor did it alter the properties of AMPH-stimulated Ca^{2+} response of the S/A-DAT-expressing cells ($n = 49–56$ cells in three independent experiments for each group, $p > 0.05$).

Proposed Mechanism of the Differential Effects of AMPH and METH on DAT—Our data support a model that METH interacts with DAT to promote a significant increase in the amount of DA efflux and Ca^{2+} release compared with the widely studied psychostimulant AMPH. Indeed, our present and past work show that N-terminal phosphorylation is important for DA efflux (26) and is needed for METH to elicit a greater release of Ca^{2+} from internal stores than AMPH. Recently, Foster *et al.* (64) have shown that distinct subpopulations of DAT exist. Importantly, these DAT populations exhibited different basal phosphorylation levels, and phorbol 12-myristate 13-acetate differentially stimulated phosphorylation of these DAT subpopulations. Consistent with these findings, we have found that unlike AMPH, METH-occupied DAT has a slower diffusion rate and lower mobile fraction.[4] Our data show that the removal of N-terminal phosphorylation sites (S/A-YFP-DAT) restored the diffusion rate of METH-occupied transporter to levels similar to control and AMPH-occupied levels, recapitulating the results obtained from calcium experiments reported here. These data taken together support a model that, via a phosphorylation-dependent process, METH and AMPH could target distinct subpopulations of DAT to stimulate a DAT-mediated increase in intracellular Ca^{2+} and DA efflux (Fig. 10).

DISCUSSION

This study provides a number of novel insights regarding the differential impact of METH *versus* AMPH on DAT functions, all of which could be molecular contributors to the addictive potential of METH compared with AMPH. First, METH evoked a greater efflux of DA via DAT than AMPH, and at a lower membrane potential (Figs. 3 and 4). This greater effect of METH on DAT function was paralleled *in vivo*, as revealed by chronomicroamperometry in the nucleus accumbens (Fig. 5). We have shown previously that DA efflux through DAT

[4] H. Khoshbouei and J. S. Goodwin, unpublished data.

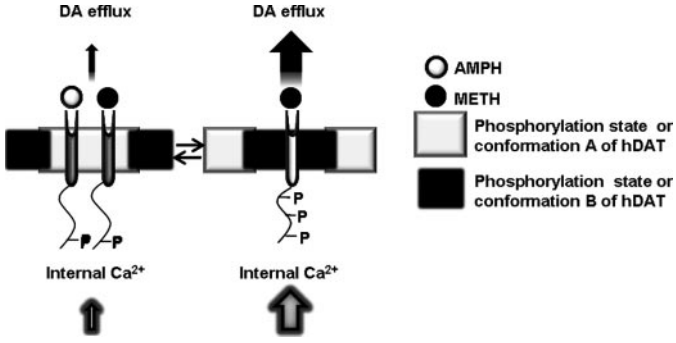

FIGURE 10. **METH and AMPH target distinct populations of DAT to stimulate a DAT-mediated increase in $[Ca^{2+}]_i$ and DA efflux.** Multiple phosphorylation/conformation states of DAT could exist. Two examples of these possible DAT populations are shown here. AMPH targets population A to stimulate DA efflux and $[Ca^{2+}]_i$ release. METH targets population B of DAT that is an activity-permissive population to stimulate DA efflux and $[Ca^{2+}]_i$ release.

requires an increase in Ca^{2+} (26). Interestingly, in this study we found that METH evokes a greater increase in $[Ca^{2+}]_i$ than AMPH (Fig. 6), although both agents elevated $[Ca^{2+}]_i$ via release of Ca^{2+} from intracellular stores (Fig. 7) in a manner that was independent of changes in membrane potential (Fig. 8). The markedly greater increase in $[Ca^{2+}]_i$ evoked by METH was entirely eliminated by mutation of the N terminus of DAT to eliminate phosphorylation of the transporter at the N-terminal region. The additive effects of PKC and of CaMKII inhibitors to suppress METH and AMPH-evoked $[Ca^{2+}]_i$ suggest that both catalysts were involved in substrate-activated $[Ca^{2+}]_i$ elevations, but that sites in the N terminus of DAT must be uniquely involved in the effects of METH and AMPH on this system. These findings suggest that the N-terminal domain of DAT contributes to the unique regulation of DAT and its functions by these two agents.

Our data provide quantification of the currents generated by forward (uptake) and reverse (efflux) translocation of DA through DAT, and are based on our ability to measure DA-induced currents under voltage clamp concurrently, as reported previously for *Xenopus* oocytes (24). The properties of DA-induced currents through DAT were dependent on whether DA was inside or outside of the cell (Fig. 2). In agreement with previous findings, outward movements of DA along with co-transported ions generated currents, which increased at depolarizing potentials (33). However, when DA was outside the cells, inward currents increased at hyperpolarizing potentials, an indication of DA uptake. Thus, the biophysical properties of DAT, including the direction of DA translocation (Fig. 2), were regulated by membrane potential, which may account for some of the published differences in the relative effects of METH *versus* AMPH on this process, because membrane potential was not always uniformly controlled in previous studies (5, 10, 14, 20–23).

Two independent states of DAT activity are likely involved in DAT-mediated DA efflux as follows: a slow process and a rapid (millisecond) burst of DA efflux through a channel-like mode of DAT. *Caenorhabditis elegans* DA neurons (65, 66) and mouse midbrain DA neurons (33) are consistent with an authentic channel mode of DAT under physiological conditions. We propose that METH might enhance the frequency of channel-like activity in DAT, promoting higher levels of DAT-associated currents (whole-cell and oxidative) detectable at more negative membrane potentials (Fig. 4, *A* and *B, left panels*). The different signaling pathways elicited by METH and AMPH must underlie the change in reversal potential seen in Fig. 4. However, the exact differences between the conductance pathways caused by these compounds are unknown at this time and are presently under investigation.

The resolution of our detection system is an improvement compared with previous studies, because it limits, although it cannot completely eliminate, the simultaneous effect of DA uptake, which diminishes our reported net DA efflux. An underestimation of the total METH- and AMPH-mediated DA efflux via the transporter occurs because some of the released DA is lost to the bulk solution, even in our time-resolved microamperometry measurements.

Elevated DA in the nucleus accumbens is essential to the development of drug addiction (43), and our *in vitro* studies paralleled an *in vivo* measurement of DAT function in this region of the brain. Our observation that systemic administration of 5 mg/kg METH resulted in a greater impact on DA clearance than AMPH in the nucleus accumbens of rats (Fig. 5*A*) provides additional evidence for differences between these two psychostimulants. Interestingly, we did not see these differences in DAT clearance in the dorsal striatum. We may learn in future studies that the interacting partners of DAT- or METH-induced regulation of the N-terminal domain of DAT differ in the nucleus accumbens and in the dorsal striatum, leading to the profoundly greater effects of METH in one region *versus* another. It is noteworthy that our *in vivo* voltammetry findings are contradictory with a recent report by John and Jones (21), who found a greater inhibition of DA uptake by AMPH than METH. However, the experimental procedures used in the two studies differ markedly. Perhaps most significantly, prior to measuring clearance, we locally applied DA into target regions of intact rat brain, whereas John and Jones (21) used 100-Hz electrical stimulation to induce endogenous DA release from mouse striatal slices. This study and the study by John *et al.* (21) advance our understanding of psychostimulant regulation of DAT. A recent report indicates that drugs with efflux-promoting properties like METH and AMPH are more effective at increasing extracellular DA levels than drugs such as cocaine, which merely block the transporter (67).

We previously reported a requirement for $[Ca^{2+}]_i$ for substrate-induced DA efflux (26). Elevation in $[Ca^{2+}]_i$ activates a variety of intracellular kinases that can lead to DAT phosphorylation (57, 60, 68). We found that either a CaMKII inhibitor (KN93) or a PKC inhibitor (BIM) attenuated AMPH- and METH-mediated $[Ca^{2+}]_i$ elevation, and that both inhibitors were required to maximally inhibit substrate-induced increases in $[Ca^{2+}]_i$. These results are consistent with previous findings that AMPH-induced DA efflux was decreased by a CaMKII inhibitor (53), and METH-stimulated DAT phosphorylation was decreased by a PKC inhibitor (49, 63). We extend those studies by demonstrating that both kinases may be required to optimally evoke elevations in $[Ca^{2+}]_i$ by DAT. The greater increase in $[Ca^{2+}]_i$ by METH, and its reliance on the N terminus of DAT, suggests that METH may enhance DAT-mediated

DA efflux by differentially altering the interaction between the DAT N-terminal domain and its interacting proteins (69). It is possible that via a phosphorylation-dependent process, METH and AMPH may target distinct subpopulations of the transporter, differentially affecting DAT electrical activity, DA efflux, and/or $[Ca^{2+}]_i$ elevations (Fig. 10).

In summary, our studies have revealed mechanistic differences between METH- and AMPH-mediated changes in DAT activity, DAT-mediated cellular responses, and DA clearance in the nucleus accumbens. These differences may contribute to the addictive properties of methamphetamine in particular, and also provide insight for novel therapeutic approaches to treat DAT-related drug addiction.

Acknowledgments—We thank Drs. Lee Limbird and Anne Kenworthy for their helpful suggestions and critical review of this manuscript, and Dr. Hubert Rucker for the generous donation of electrophysiology equipment.

REFERENCES

1. Giros, B., and Caron, M. G. (1993) *Trends Pharmacol. Sci.* **14,** 43–49
2. Rothman, R. B., and Baumann, M. H. (2003) *Eur. J. Pharmacol.* **479,** 23–40
3. Han, D. D., and Gu, H. H. (2006) *BMC Pharmacol.* **6,** 6
4. Fischer, J. F., and Cho, A. K. (1976) *Proc. West Pharmacol. Soc.* **19,** 179–182
5. Eshleman, A. J., Henningsen, R. A., Neve, K. A., and Janowsky, A. (1994) *Mol. Pharmacol.* **45,** 312–316
6. Wall, S. C., Gu, H., and Rudnick, G. (1995) *Mol. Pharmacol.* **47,** 544–550
7. Sitte, H. H., Huck, S., Reither, H., Boehm, S., Singer, E. A., and Pifl, C. (1998) *J. Neurochem.* **71,** 1289–1297
8. Jones, S. R., Gainetdinov, R. R., Jaber, M., Giros, B., Wightman, R. M., and Caron, M. G. (1998) *Proc. Natl. Acad. Sci. U. S. A.* **95,** 4029–4034
9. Jones, S. R., Gainetdinov, R. R., Wightman, R. M., and Caron, M. G. (1998) *J. Neurosci.* **18,** 1979–1986
10. Segal, D. S., and Kuczenski, R. (1997) *J. Pharmacol. Exp. Ther.* **282,** 561–573
11. Broom, S. L., and Yamamoto, B. K. (2005) *Psychopharmacology* **181,** 467–476
12. Johnson, R. A., Eshleman, A. J., Meyers, T., Neve, K. A., and Janowsky, A. (1998) *Synapse* **30,** 97–106
13. Hanson, G. R., Rau, K. S., and Fleckenstein, A. E. (2004) *Neuropharmacology* **47,** Suppl. 1, 92–100
14. Rothman, R. B., Baumann, M. H., Dersch, C. M., Romero, D. V., Rice, K. C., Carroll, F. I., and Partilla, J. S. (2001) *Synapse* **39,** 32–41
15. Cox, R. H., Jr., and Maickel, R. P. (1972) *J. Pharmacol. Exp. Ther.* **181,** 1–9
16. Peachey, J. E., Rogers, B., and Brien, J. F. (1977) *Psychopharmacology* **51,** 137–140
17. National Institute on Drug Abuse (2006) *NIDA Research Report*, pp. 1–8
18. Colliver, J., Kroutil, L. A., Dai, L., and Gfroerer, J. C. (2006) *Misuse of Prescription Drugs: Data from the 2002, 2003, and 2004 National Surveys on Drug Use and Health*, Substance Abuse and Mental Health Services Administration, Office of Applied Studies, Rockville, MD
19. Joyce, B. M., Glaser, P. E., and Gerhardt, G. A. (2007) *Psychopharmacology* **191,** 669–677
20. Shoblock, J. R., Sullivan, E. B., Maisonneuve, I. M., and Glick, S. D. (2003) *Psychopharmacology* **165,** 359–369
21. John, C. E., and Jones, S. R. (2007) *Neuropharmacology* **52,** 1596–1605
22. Kuczenski, R., Segal, D. S., Cho, A. K., and Melega, W. (1995) *J. Neurosci.* **15,** 1308–1317
23. Hall, D. A., Stanis, J. J., Marquez Avila, H., and Gulley, J. M. (2008) *Psychopharmacology* **195,** 469–478
24. Sonders, M. S., Zhu, S. J., Zahniser, N. R., Kavanaugh, M. P., and Amara, S. G. (1997) *J. Neurosci.* **17,** 960–974
25. Khoshbouei, H., Wang, H., Lechleiter, J. D., Javitch, J. A., and Galli, A. (2003) *J. Biol. Chem.* **278,** 12070–12077
26. Khoshbouei, H., Sen, N., Guptaroy, B., Johnson, L., Lund, D., Gnegy, M. E., Galli, A., and Javitch, J. A. (2004) *PLoS Biol.* **2,** E78
27. Kahlig, K. M., and Galli, A. (2003) *Eur. J. Pharmacol.* **479,** 153–158
28. Hastrup, H., Karlin, A., and Javitch, J. A. (2001) *Proc. Natl. Acad. Sci. U. S. A.* **98,** 10055–10060
29. Hastrup, H., Sen, N., and Javitch, J. A. (2003) *J. Biol. Chem.* **278,** 45045–45048
30. Rees, S., Coote, J., Stables, J., Goodson, S., Harris, S., and Lee, M. G. (1996) *BioTechniques* **20,** 102–104, 106, 108–110
31. Robbins, A. K., and Horlick, R. A. (1998) *BioTechniques* **25,** 240–244
32. Kahlig, K. M., Javitch, J. A., and Galli, A. (2004) *J. Biol. Chem.* **279,** 8966–8975
33. Kahlig, K. M., Binda, F., Khoshbouei, H., Blakely, R. D., McMahon, D. G., Javitch, J. A., and Galli, A. (2005) *Proc. Natl. Acad. Sci. U. S. A.* **102,** 3495–3500
34. Zahniser, N. R., Dickinson, S. D., and Gerhardt, G. A. (1998) *Methods Enzymol.* **296,** 708–719
35. Gulley, J. M., Everett, C. V., and Zahniser, N. R. (2007) *Brain Res.* **1151,** 32–45
36. Paxinos, G., and Watson, C. (1998) *The Rat Brain in Stereotaxic Coordinates*, Academic Press, San Diego
37. Fujimoto, Y., Kitaichi, K., Nakayama, H., Ito, Y., Takagi, K., and Hasegawa, T. (2007) *Exp. Anim.* **56,** 119–129
38. Kitaichi, K., Morishita, Y., Doi, Y., Ueyama, J., Matsushima, M., Zhao, Y. L., Takagi, K., and Hasegawa, T. (2003) *Eur. J. Pharmacol.* **464,** 39–48
39. Riviere, G. J., Gentry, W. B., and Owens, S. M. (2000) *J. Pharmacol. Exp. Ther.* **292,** 1042–1047
40. Garcia, B. G., Wei, Y., Moron, J. A., Lin, R. Z., Javitch, J. A., and Galli, A. (2005) *Mol. Pharmacol.* **68,** 102–109
41. Cass, W. A., Gerhardt, G. A., Gillespie, K., Curella, P., Mayfield, R. D., and Zahniser, N. R. (1993) *J. Neurochem.* **61,** 273–283
42. Zahniser, N. R., Negri, C. A., Hanania, T., and Gehle, V. M. (1999) *Alcohol Clin. Exp. Res.* **23,** 1721–1729
43. Kalivas, P. W., Volkow, N., and Seamans, J. (2005) *Neuron* **45,** 647–650
44. Chan, S. L., Liu, D., Kyriazis, G. A., Bagsiyao, P., Ouyang, X., and Mattson, M. P. (2006) *J. Biol. Chem.* **281,** 37391–37403
45. Kapur, N., Mignery, G. A., and Banach, K. (2007) *Am. J. Physiol.* **292,** C1510–C1518
46. Lytton, J., Westlin, M., and Hanley, M. R. (1991) *J. Biol. Chem.* **266,** 17067–17071
47. Awatramani, G. B., Price, G. D., and Trussell, L. O. (2005) *Neuron* **48,** 109–121
48. Lucaj, Z., and Fujii, J. T. (1994) *Brain Res.* **660,** 1–7
49. Cervinski, M. A., Foster, J. D., and Vaughan, R. A. (2005) *J. Biol. Chem.* **280,** 40442–40449
50. Foster, J. D., Pananusorn, B., and Vaughan, R. A. (2002) *J. Biol. Chem.* **277,** 25178–25186
51. Vaughan, R. A. (2004) *J. Pharmacol. Exp. Ther.* **310,** 1–7
52. Kantor, L., Hewlett, G. H., Park, Y. H., Richardson-Burns, S. M., Mellon, M. J., and Gnegy, M. E. (2001) *J. Pharmacol. Exp. Ther.* **297,** 1016–1024
53. Fog, J. U., Khoshbouei, H., Holy, M., Owens, W. A., Vaegter, C. B., Sen, N., Nikandrova, Y., Bowton, E., McMahon, D. G., Colbran, R. J., Daws, L. C., Sitte, H. H., Javitch, J. A., Galli, A., and Gether, U. (2006) *Neuron* **51,** 417–429
54. Foster, J. D., Pananusorn, B., Cervinski, M. A., Holden, H. E., and Vaughan, R. A. (2003) *Brain Res. Mol. Brain Res.* **110,** 100–108
55. Giambalvo, C. T. (1988) *Biochem. Pharmacol.* **37,** 4009–4017
56. Giambalvo, C. T. (1989) *Biochem. Pharmacol.* **38,** 4445–4454
57. Gorentla, B. K., and Vaughan, R. A. (2005) *Neuropharmacology* **49,** 759–768
58. Sandoval, V., Riddle, E. L., Ugarte, Y. V., Hanson, G. R., and Fleckenstein, A. E. (2001) *J. Neurosci.* **21,** 1413–1419
59. Vaughan, R. A., Huff, R. A., Uhl, G. R., and Kuhar, M. J. (1997) *J. Biol. Chem.* **272,** 15541–15546
60. Doolen, S., and Zahniser, N. R. (2001) *J. Pharmacol. Exp. Ther.* **296,** 931–938

61. Huff, R. A., Vaughan, R. A., Kuhar, M. J., and Uhl, G. R. (1997) *J. Neurochem.* **68,** 225–232
62. Browman, K. E., Kantor, L., Richardson, S., Badiani, A., Robinson, T. E., and Gnegy, M. E. (1998) *Brain Res.* **814,** 112–119
63. Kantor, L., and Gnegy, M. E. (1998) *J. Pharmacol. Exp. Ther.* **284,** 592–598
64. Foster, J. D., Adkins, S. D., Lever, J. R., and Vaughan, R. A. (2008) *J. Neurochem.* **105,** 1683–1699
65. Carvelli, L., Blakely, R. D., and Defelice, L. J. (2008) *Proc. Natl. Acad. Sci. U. S. A.*, **105,** 14192–14197
66. Carvelli, L., McDonald, P. W., Blakely, R. D., and Defelice, L. J. (2004) *Proc. Natl. Acad. Sci. U. S. A.* **101,** 16046–16051
67. Salahpour, A., Ramsey, A. J., Medvedev, I. O., Kile, B., Sotnikova, T. D., Holmstrand, E., Ghisi, V., Nicholls, P. J., Wong, L., Murphy, K., Sesack, S. R., Wightman, R. M., Gainetdinov, R. R., and Caron, M. G. (2008) *Proc. Natl. Acad. Sci. U. S. A.* **105,** 4405–4410
68. Doolen, S., and Zahniser, N. R. (2002) *FEBS Lett.* **516,** 187–190
69. Torres, G. E., Gainetdinov, R. R., and Caron, M. G. (2003) *Nat. Rev. Neurosci.* **4,** 13–25